Numerical Simulations of Draw Resonance in Melt Spinning of Polymer Fluids

JINAN CAO*

Department of Organic and Polymeric Materials, Tokyo Institute of Technology, Tokyo, Japan

SYNOPSIS

This article deals with numerical simulations of draw resonance of polymer fluids by employing direct difference methods to solving the governing equations in melt spinning. The stability of each difference method was studied by a comparison of the results obtained from simulations with the theoretical solutions or values. The numerical simulation confirms that the critical draw ratio of draw resonance in an isothermal and uniform tension spinning of a Newtonian fluid is between 20 and 21. The cross-sectional area of a spinline in draw resonance was found to decrease monotonically from a spinneret toward a take-up bobbin, although the taken-up filament shows periodical variation. This study has also illustrated the mechanism of draw resonance previously proposed by the author. © 1993 John Wiley & Sons, Inc.

INTRODUCTION

Draw resonance of polymer fluids is a characteristic instability in melt spinning and film-forming processes and has been the subject of extensive research.[1-17] This instability, being of importance in both polymer engineering and polymer science, not only reflects the changes in rheological properties of a polymer fluid, but also reveals information on the molecular structure formation of the fluid in melt spinning. Furthermore, it has been pointed out by the author that draw resonance in melt spinning and the instability of polymers in tensile testing share the same mechanism because of the similarities in their physical and mathematical models.[18] This finding has permitted a transfer of many concepts and ideas developed from studies on draw resonance in melt spinning to the tensile testing instability, which is a general concern in materials science.

In a previous paper,[17] the author proposed that the nonuniformizing draw mode is the necessary condition of draw resonance and the mechanism of draw resonance lies in the positive feedback feature of a spinline with the nonuniformizing draw mode to a turbulence. To further demonstrate and illustrate this mechanism, a profile simulation of the spinline in draw resonance is desirable.

On the other hand, to elucidate the mechanism of fiber structure formation in melt spinning, the mathematical model of melt spinning has been extensively studied. The governing equations of melt spinning were established in the 1960s. They consist of simultaneous nonlinear partial differential equations and cannot be solved analytically except in a few special cases. Numerical methods have to be employed and their results have played an important role in interpreting the mechanism of molecular structure formation of polymers in melt spinning.[19,20]

To obtain the critical draw ratio of draw resonance of polymer fluids in melt spinning, a linearized perturbation approximation of the governing equations has been usually adopted. An orthogonal collocation method to solving the simultaneous nonlinear partial differential equations was also found to be useful in obtaining the critical draw ratio of draw resonance.[21] These methods are valid and helpful, but cannot be utilized for the simulations of spinline profiles and the exact wave form of the diameter of taken-up filament in a unsteady state.

Ishihara and Kase reported a direct difference method to solve the governing equations without

* Present address: CSIRO Division of Wool Technology, P.O. Box 21, Belmont, Victoria 3216, Australia.

Journal of Applied Polymer Science, Vol. 49, 1759-1768 (1993)
 CCC 0021-8995/93/101759-10

recourse to the perturbation approximation to acquire the critical draw ratio of draw resonance.[13,22] However, the spinline profile in draw resonance was not obtained.

The purpose of this paper is to further demonstrate and illustrate the mechanism of draw resonance by numerical simulations of the spinline profiles in draw resonance, using a Newtonian fluid as an example. The stabilities of various difference schemes were first compared. The critical draw ratio for a Newtonian fluid and the spinline profile in draw resonance were then simulated.

NONDIMENSIONAL GOVERNING EQUATIONS AND FINITE DIFFERENCE METHODS

Nondimensional Governing Equations and Boundary Conditions

The governing equations of isothermal melt spinning consist of the following constitution equation and continuity equation:

$$\frac{\partial v}{\partial x} = \frac{F}{A\beta} \tag{1}$$

$$\frac{\partial A}{\partial t} + \frac{\partial (Av)}{\partial x} = 0 \tag{2}$$

where A and v denote, respectively, the cross-sectional area and velocity of a filament at time t and distance x from a spinneret. The symbol F represents the spinning tension and is a constant along a spinline but variable with time t by the definition of uniform tension spinning. β is the Trouton extensional viscosity.

Only the strain rate dependence of the Trouton viscosity is considered. For a power law polymer fluid, it is written as

$$\beta = \beta_0 \left(\frac{\partial v}{\partial x} \right)^{p-1} \tag{3}$$

where β_0 is a viscosity constant, and the superscript p, a parameter expressing the strain rate dependence of the Trouton viscosity. When p tends to unity, a Newtonian fluid is obtained. In this study, only Newtonian fluids will be addressed.

These equations can be expressed in terms of nondimensional variables in order to increase generality and reduce the arithmetical procedures involved in a simulation:

$$\frac{\partial \psi}{\partial \zeta} = \left(\frac{\xi}{\lambda} \right) \tag{4}$$

$$\frac{\partial \lambda}{\partial \tau} + \frac{\partial (\lambda \psi)}{\partial \zeta} = 0 \tag{5-1}$$

The continuity equation eq. (5-1) has another form, which is completely equivalent to eq. (5-1) for an analytical solution:

$$\frac{\partial \lambda}{\partial \tau} + \psi \frac{\partial \lambda}{\partial \zeta} + \xi = 0 \tag{5-2}$$

where λ and ψ denote, respectively, the nondimensional cross-sectional area and velocity of a filament at nondimensional distance ζ from a spinneret and nondimensional time, τ. The symbol ξ is the nondimensional spinning tension.

These nondimensional parameters are defined as follows:

$\zeta = x/L$	nondimensional spinline distance from a spinneret
$\tau = tV_0/L$	nondimensional time
$\lambda = A/A_0$	nondimensional cross-sectional area of a filament
$\psi = v/V_0$	nondimensional velocity of a filament
$\xi = [F/(A_0\beta_0)] \times (L/V_0)$	nondimensional spinning tension

where, L, A_0, and V_0 are the distance from a spinneret to a take-up bobbin, the cross-sectional area, and the extrusion rate at the spinneret, respectively.

The nondimensional boundary and initial conditions can be written as

$$\psi = 1, \quad \text{where } \zeta = 0 \tag{6}$$

$$\psi = \psi_w, \quad \text{where } \zeta = 1 \tag{7}$$

and where ψ_w is the draw ratio of a spinning.

The nondimensional distance, ζ, may be transformed to the nondimensional resident time, ζ^*, of a polymer fluid traveling from a spinneret to this distance that is defined in eq. (8):

$$\zeta^* = \int_0^\zeta \frac{d\zeta}{\psi} \tag{8}$$

The nondimensional variables ζ and ζ^* are equivalent in a steady state since they have a one-

to-one corresponding relationship. In an unsteady state, however, it is difficult to determine the boundary condition corresponding to $\zeta = 1$ by using the nondimensional resident time, ζ^*, because the resident time of a polymer fluid from the spinneret to the take-up point varies. The transformation of the variable ζ to the variable ζ^* increases difficulties in arithmetic involved in a simulation. In some papers, the boundary condition for an unsteady state has been set as[13,22]

$$\zeta_w^* = \int_0^1 \frac{d\zeta}{\psi_0} \tag{9}$$

where ψ_0 is the nondimensional velocity of a filament in a steady state.

It should be pointed out that this treatment is applicable only in a steady state of spinning and could result in a potential systematic error in the numerical simulations of a unsteady state. In this present study, the nondimensional variables of time τ and distance ζ are employed as the independent variables of the governing equations.

Difference Equations of the Governing Equations

The convergence and stability of a difference method are very important when the method is applied to solving a nonlinear partial differential equation. On the other hand, a definite theory on the convergence and stability has not been established. It is a common practice that one investigates whether a difference method is convergent and stable or not by comparing the solution derived from the difference method with a theoretical or physical solution, if this solution is obtainable.

Figure 1 shows two various difference schemes applicable to solving the nondimensional governing equations with the above-mentioned boundary and initial conditions. From here on, the schemes in Figure 1(A) for eqs. (4) and (5-1), (4), and (5-2) are called Method A and Method B, respectively, while the scheme of Figure 1(B) for eqs. (4) and (5-1) is termed Method C. The comparison of Methods A and C shows the effect of the difference schemes on the stability of a numerical solution, and the comparison of Methods A and B should indicate the effect of partial differential equation forms, i.e., eqs. (5-1) and (5-2), on the stability, although they are completely equivalent in an analytical solution.

The difference equations of Methods A, B, and C for a Newtonian fluid are written as

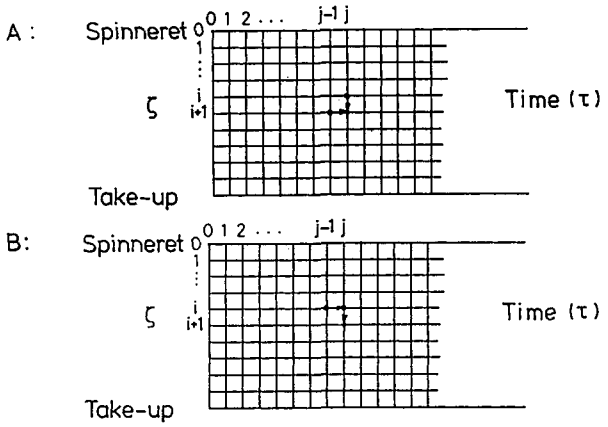

Figure 1 Difference schemes employed in this study.

Method A:

$$\psi_{i+1,j} = \psi_{i,j} + \xi_{i,j}\frac{\Delta\zeta}{\lambda_{i,j}} \tag{10}$$

$$\lambda_{i+1,j} = \frac{\lambda_{i+1,j-1} + \omega\lambda_{i,j}\psi_{i,j}}{1 + \omega\psi_{i+1,j}} \tag{11}$$

Method B:

$$\psi_{i+1,j} = \psi_{i,j} + \xi_{i,j}\frac{\Delta\zeta}{\lambda_{i,j}} \tag{12}$$

$$\lambda_{i+1,j} = \frac{-\xi_{i,j}\omega\Delta\zeta + \lambda_{i+1,j-1} + \omega\lambda_{i,j}\psi_{i,j}}{1 + \omega\psi_{i,j}} \tag{13}$$

and Method C:

$$\psi_{i+1,j} = \psi_{i,j} + \xi_{i,j}\frac{\Delta\zeta}{\lambda_{i,j}} \tag{14}$$

$$\lambda_{i+1,j} = \frac{1}{\omega\psi_{i+1,j}}\{\omega\lambda_{i,j}\psi_{i,j} - (\lambda_{i,j} - \lambda_{i,j-1})\} \tag{15}$$

where $\omega = \Delta\tau/\Delta\zeta$ represents the mesh ratio of a difference scheme.

RESULTS AND DISCUSSION

Simulation of Isothermal Spinning under Uniform Stress

With isothermal melt spinning under uniform stress, the ratio of the spinning tension and the cross-sectional area of a filament is a constant along the spinline but may vary with time by the definition. In such spinning for a power law polymer fluid in-

cluding a Newtonian fluid, the governing equations have an analytical solution, given that the spinning conditions are maintained constant[17]:

$$\lambda(\zeta, \tau) = \frac{1}{(\psi_w - 1)\zeta + 1} \tag{16}$$

$$\psi(\zeta, \tau) = (\psi_w - 1)\zeta + 1 \tag{17}$$

This solution indicates that a constant diameter of filament will be observed whenever the spinning conditions are maintained unvariable. This analytical solution can be used for the comparison with numerical solutions. The stability of a difference scheme can then be discussed based on this comparison.

The numerical simulation for such a spinning was performed by assuming that the take-up velocity has a 10% step increment at nondimensional time 0; then, the new take-up velocity is kept unvariable. The mathematical expression for this step increment of the take-up velocity can be written

$$\psi(1, \tau) = \begin{cases} \psi_w & \text{when } \tau \leqq 0 \\ 1.1\psi_w & \text{when } \tau > 0 \end{cases} \tag{18}$$

The other initial and boundary conditions are

$$\lambda(\zeta, 0) = \frac{1}{(\psi_w - 1)\zeta + 1} \tag{19}$$

$$\psi(\zeta, 0) = (\psi_w - 1)\zeta + 1 \tag{20}$$

$$\psi(0, \tau) = 1 \tag{21}$$

$$\lambda(0, \tau) = 1 \tag{22}$$

To facilitate calculation forwardly from a spinneret to a take-up point, the nondimensional spinning tension, ξ (in this section, the nondimensional spinning stress, i.e., ξ/λ), has to be given a tentative value. By comparing the calculated take-up velocity, $\psi[1, \tau(j)]$, with the real take-up velocity, $1.1\psi_w$, one reiterates the revision of the nondimensional spinning tension by employing the following Newtonian interpolation method until the calculated take-up velocity becomes satisfactory:

$$\xi_j^{(k+2)} = \frac{e^{(k+1)}\xi_j^{(k)} - e^{(k)}\xi_j^{(k+1)}}{e^{(k+1)} - e^{(k)}} \tag{23}$$

$$e^{(k)} = \psi[1, \tau(j)^{(k)}] - 1.1\psi_w$$

$$k = 1, 2, 3, \ldots \tag{24}$$

where ξ_j denotes the nondimensional spinning tension at the nondimensional time $\tau = j$, and $\xi_j^{(1)}$ and $\xi_j^{(2)}$ are, respectively, the first and second tentative values of the nondimensional spinning tension at time j. $e^{(k)}$ represents the difference between the calculated and real take-up velocities. The interpolation was iterated until the difference became less than 1/1,000,000 of the real take-up velocity. The above-mentioned initial and boundary conditions, as well as the Newtonian interpolation method, are also adopted in the following two sections.

Figure 2 shows the simulated responses of the nondimensional cross-sectional area of a taken-up filament using Method A to the 10% step increment of the take-up velocity. It is observed that the numerical solutions converge to the analytical solutions in all the draw ratios employed, except in the region

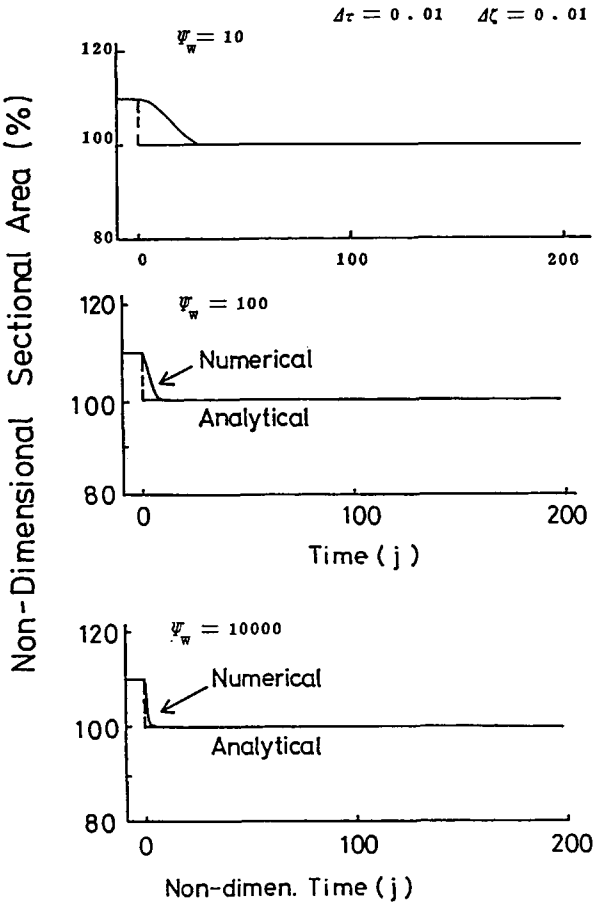

Figure 2 The responses of the cross-sectional area of taken-up filament to the step increment of the take-up velocity simulated using Method A for an isothermal spinning of a power law polymer fluid under uniform stress.

close to the discontinuous point of the step increment. The nondimensional cross-sectional area was rescaled in this figure so that 100% represented the cross-sectional area in the steady state corresponding to the new take-up velocity after the 10% step increment.

The numerical solutions using Method B are shown in Figure 3. A draw ratio of 100 was adopted in these simulations. It is clear from the figure that the numerical solutions diverge from the analytical solutions, suggesting that Method B has a poor stability although the error becomes smaller as the mesh is divided finely. A significant error could be still observed even in the case of $\Delta\tau = 0.005$ and $\Delta\zeta = 0.0025$. Therefore, this method is not favored.

The responses of the nondimensional cross-sectional area of taken-up filament to the 10% step

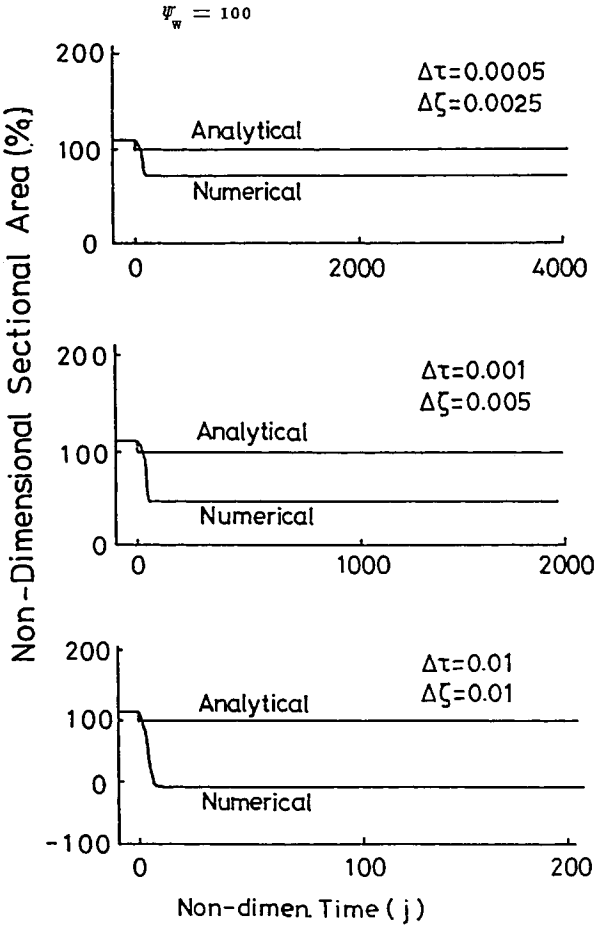

Figure 3 The responses of the cross-sectional area of taken-up filament to the step increment of the take-up velocity simulated using Method B for an isothermal spinning of a power law polymer fluid under uniform stress.

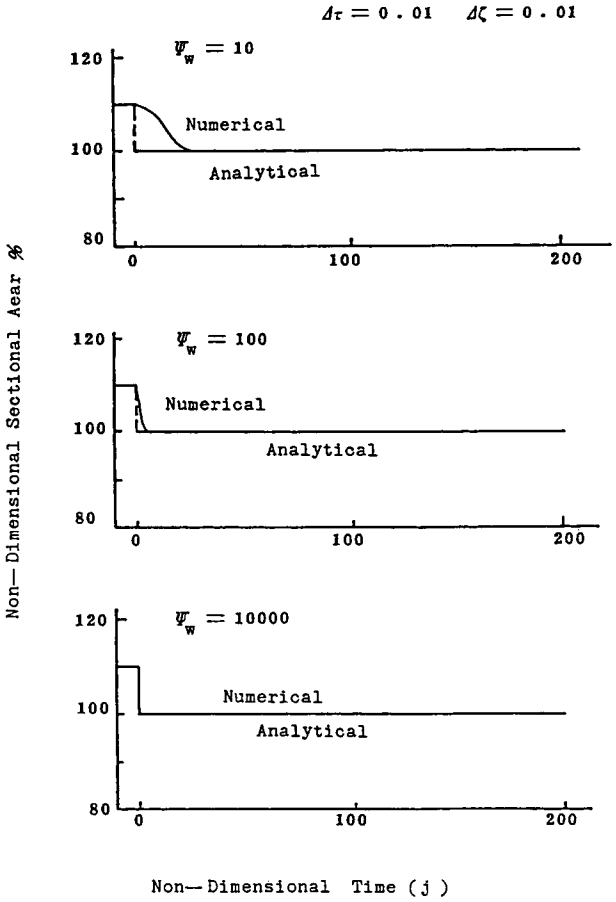

Figure 4 The responses of the cross-sectional area of taken-up filament to the step increment of the take-up velocity simulated using Method C for an isothermal spinning of a power law polymer fluid under uniform stress.

increment of the taken-up velocity, simulated using Method C, are displayed in Figure 4. The mesh adopted in the simulation was $\Delta\tau = \Delta\zeta = 0.01$. The numerical solutions are found not only to converge to the analytical solutions in all the draw ratios employed, but also to have a faster convergence rate than that of Method A, indicating that Method C could be the best of the three methods.

The Critical Draw Ratio of Isothermal and Uniform Tension Spinning for a Newtonian Fluid

Draw resonance occurs in isothermal and uniform tension spinning of a Newtonian fluid as the draw ratio exceeds the critical draw ratio 20.218.[23] In such a spinning, no analytical solution could be obtained. Figure 5 shows the responses of the cross-sectional area of the taken-up filament to the 10% step in-

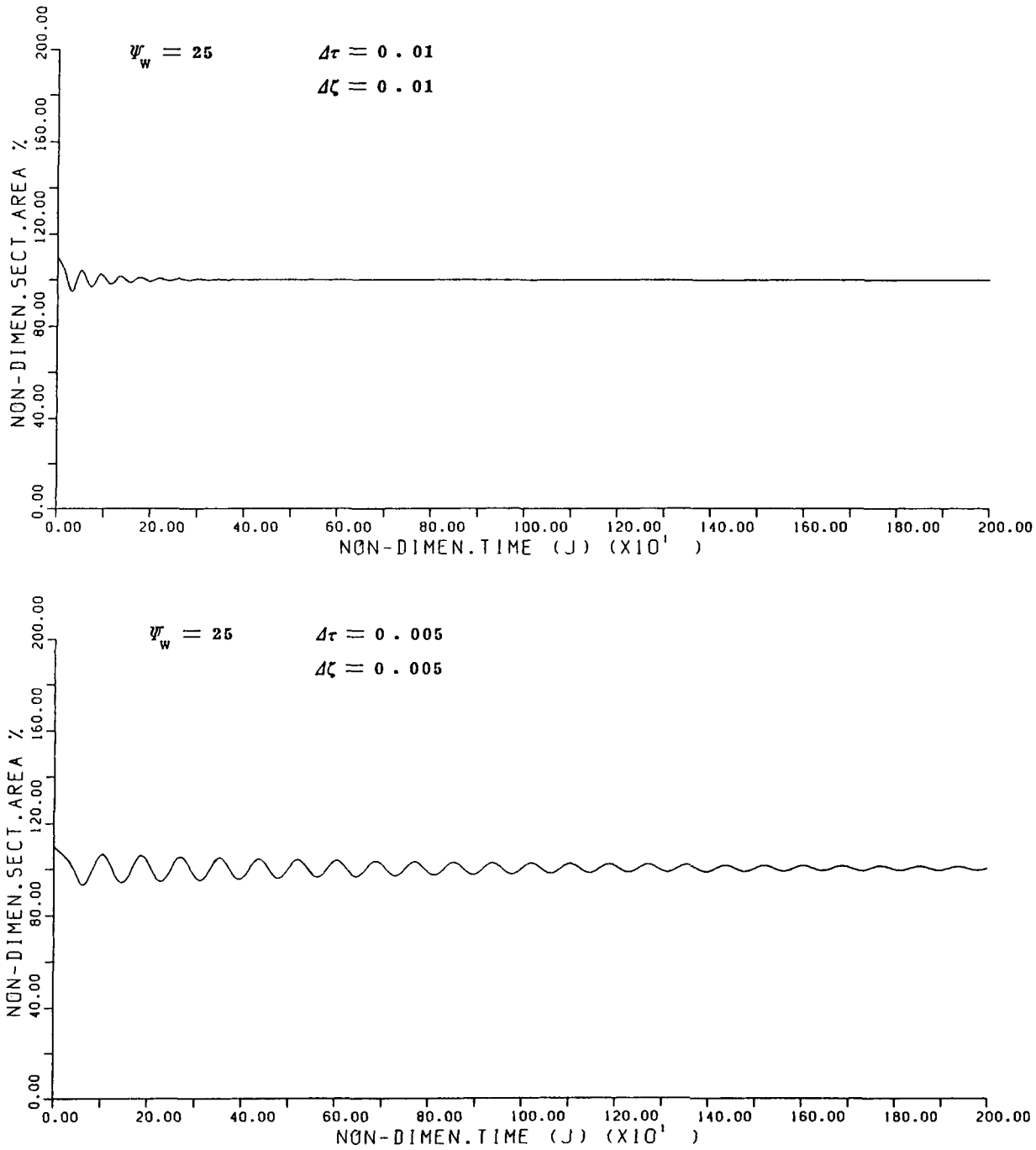

Figure 5 The responses of the cross-sectional area of taken-up filament to the step increment of the take-up velocity, simulated using Method A for an isothermal and uniform tension spinning of a Newtonian fluid: (a) $\Delta\tau = \Delta\zeta = 0.01$; (b) $\Delta\tau = \Delta\zeta = 0.005$.

crement of the take-up velocity, computed using Method A. It is observed in this figure that the cross-sectional area approaches a steady value in spite of the draw ratio of 25. This contradiction could result from the stability of the difference equations in such a spinning. The responses of the cross-sectional area simulated using Method B are represented in Figure 6. The cross-sectional area of the taken-up filament is found to approach a steady value after a short period of transient time diverging from 100%. This value of 100% should be the analytical solution from a physical viewpoint, suggesting that the stability

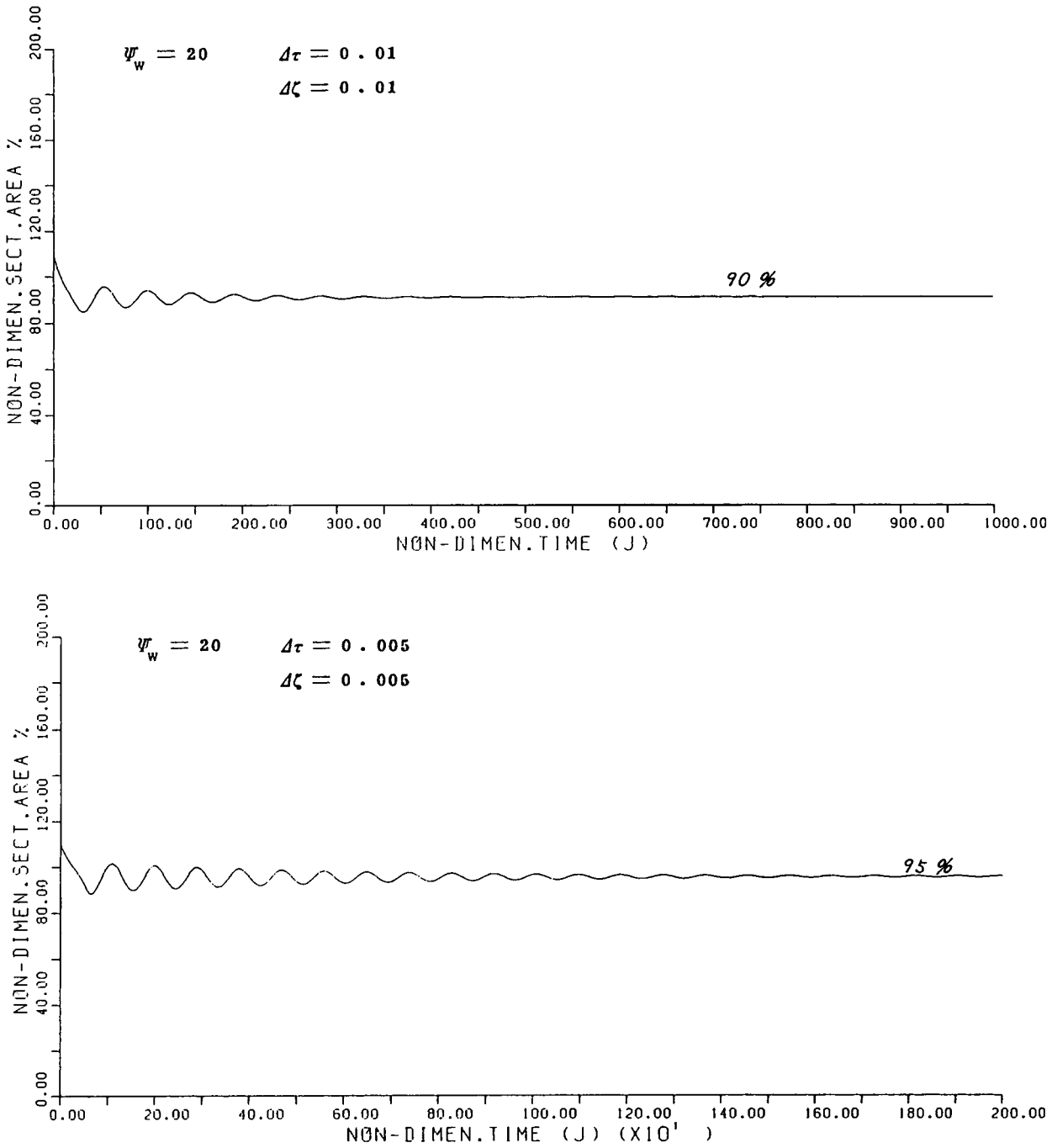

Figure 6 The responses of the cross-sectional area of taken-up filament to the step increment of the take-up velocity, simulated using Method B for an isothermal and uniform tension spinning of a Newtonian fluid: (a) $\Delta\tau = \Delta\zeta = 0.01$; (b) $\Delta\tau = \Delta\zeta = 0.005$.

of Method B in such a spinning is also poor. Both Methods A and B show improvements in approaching the theoretical values as the meshes are finely divided.

Displayed in Figure 7 are the responses of the cross-sectional area of the taken-up filament to the 10% step increment of the take-up velocity, simulated using Method C. The cross-sectional area approaches a steady value in the case of the draw ratio of 20, whereas a sustained variation with a standing period and amplitude is maintained as the draw ratio is increased to 21, suggesting that the critical draw

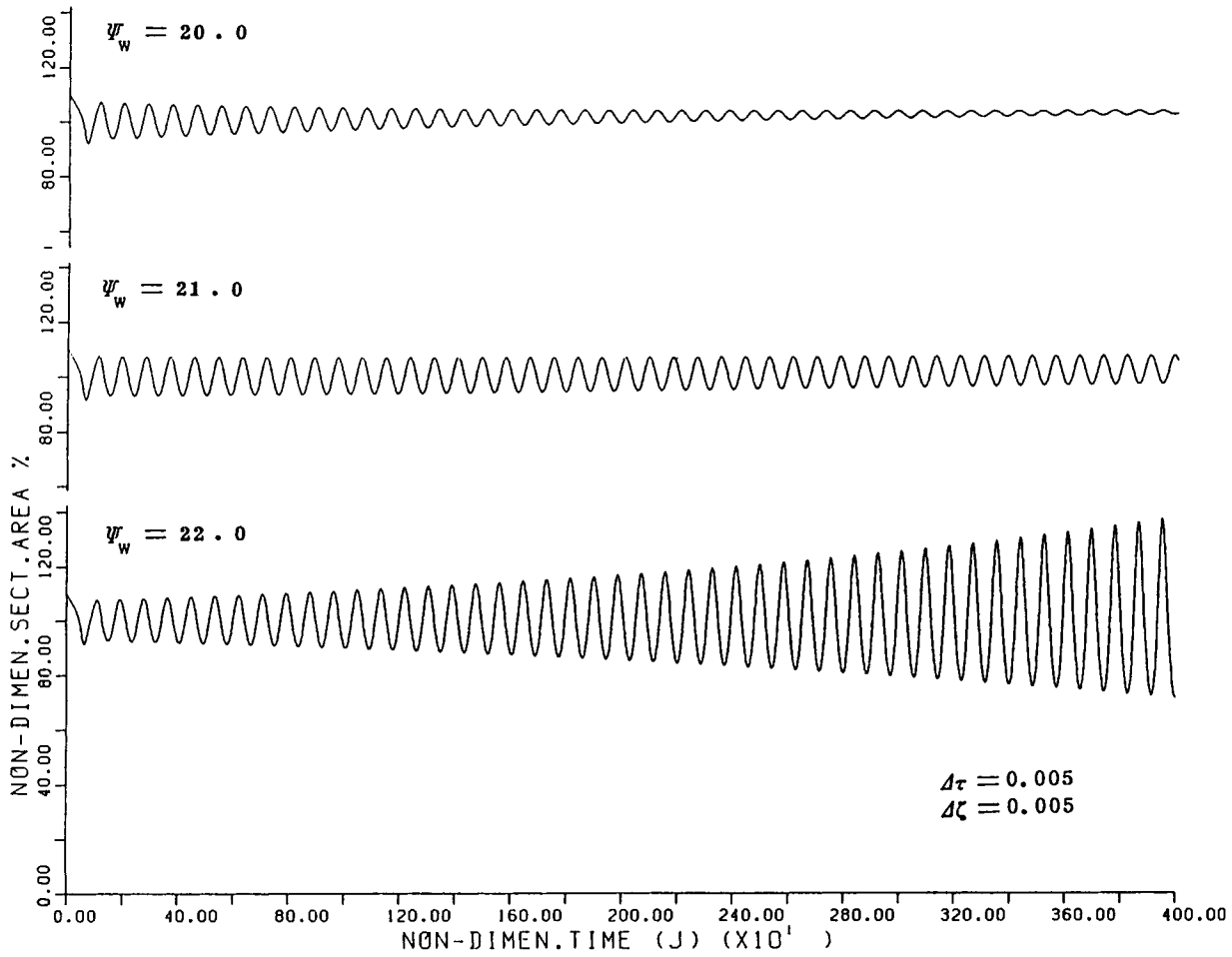

Figure 7 The responses of the cross-sectional area of taken-up filament to the step increment of the take-up velocity, simulated using Method C for an isothermal and uniform tension spinning of a Newtonian fluid.

ratio of draw resonance in such a spinning lies between 20 and 21. This value is consistent with the reported theoretical value of 20.218.[23] The critical draw ratio was identified to be only between 7.4 and 20.1 by using a direct difference method to solve the governing equations in such a spinning in the literature.[13,22] This present simulation, therefore, could be regarded as a reliable numerical method with high stability.

Spinline Profiles in Draw Resonance

The spinline profiles in draw resonance were simulated by employing Method C and assuming an isothermal and uniform tension spinning of a Newtonian fluid at the draw ratio of 50. Figure 8 illustrates the response of the nondimensional cross-sectional area of taken-up filament to the 10% step increment of the take-up velocity. After a transient period, the cross-sectional area of taken-up filament approaches a sustained limit cycle oscillating with a standing period and amplitude. Since the draw ratio of 50 is much higher than the critical draw ratio of 20.218, the wave form is found to be very sharp.

The spinline profiles of one cycle corresponding to the nondimensional time 363–428 in Figure 8 are presented in Figure 9. It is clear from this figure that the nondimensional cross-sectional area of the spinlines decreases monotonically from the spinneret to the take-up bobbin in spite of the cross-sectional area of taken-up filament varying with a standing period and amplitude as draw resonance occurs.

Figure 9 also visualizes how a spinning fluid is attenuated along a spinline in draw resonance. The two small volumes of the spinning fluid in Figure 9, represented by A and B, descend at almost the same

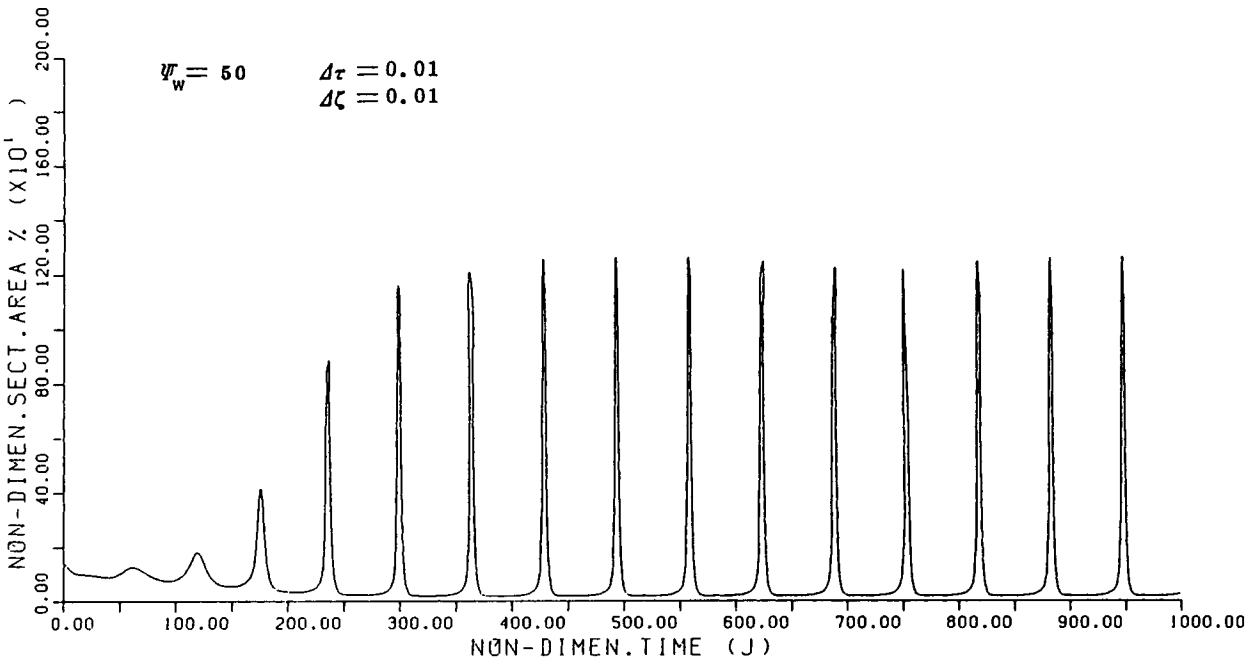

Figure 8 The responses of the cross-sectional area of taken-up filament to the step increment of the take-up velocity, simulated using Method C for an isothermal and uniform tension spinning of a Newtonian fluid; draw ratio = 50.

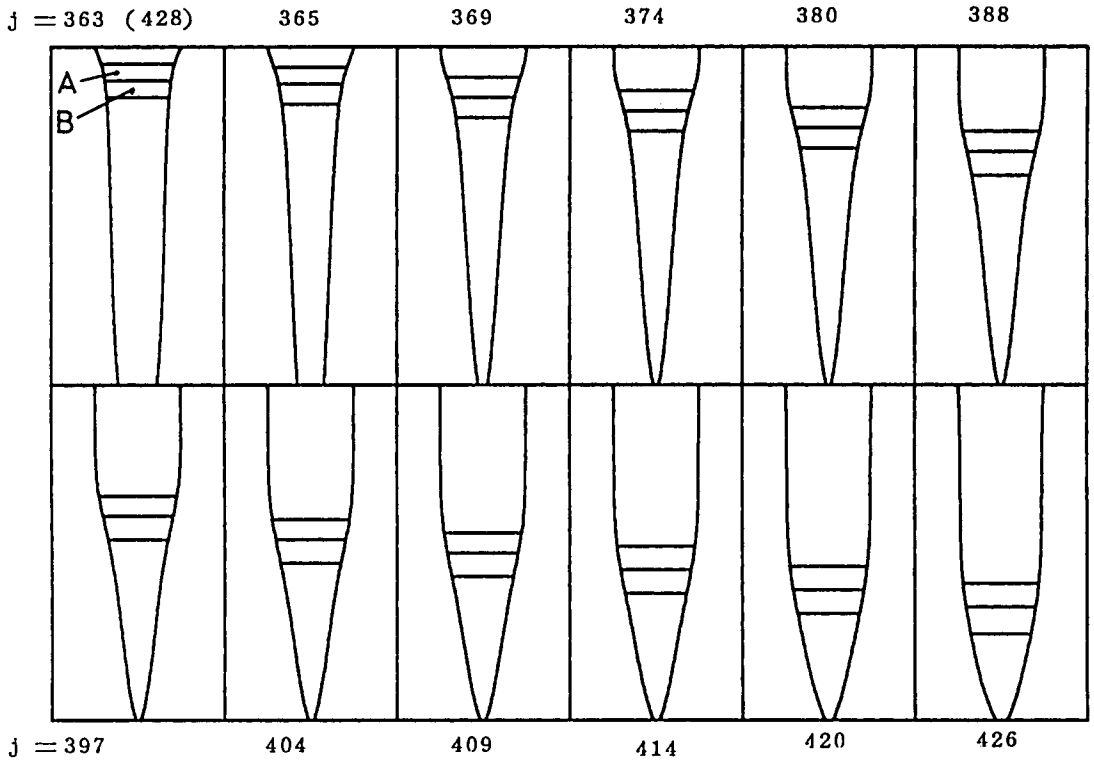

Figure 9 Spinline profiles in draw resonance. One cycle corresponding to the nondimensional time 363–426.

velocity as the extruding velocity from the nondimensional time 363 to 426. Little attenuation of the small volumes could be observed. Attenuation is found to concentrate at the thinner parts of the spinline. Only in the final moment were the small volumes accelerated to meet the take-up velocity, resulting in the peak at the nondimensional time 428 in Figure 8. This simulation, therefore, demonstrated and illustrated directly the mechanism of draw resonance proposed by the author.[17] It should be mentioned that this feature of draw resonance observed in Figure 9 is believed not to be a specific feature for a Newtonian fluid in such a spinning, but to be the common feature of draw resonance for polymer fluids.

CONCLUSION

It has been found that both the form of the governing equations and the finite difference schemes are relevant to the stability of a numerical simulation of melt spinning. This study suggests that the governing equations, eqs. (4) and (5-1), and the forward difference scheme A have the highest stability in the simulations of draw resonance. The critical draw ratio of draw resonance for a Newtonian fluid in an isothermal and uniform tension spinning is confirmed to lie between 20 and 21 by using the direct difference method. The cross-sectional area of a spinline in draw resonance was found to decrease monotonically from a spinneret toward a take-up bobbin in spite of the taken-up filament showing variation with a standing period and amplitude. This simulation is believed to have demonstrated and illustrated directly the mechanism of draw resonance proposed by the author.

APPENDIX

The numerical computations were performed by using an M-280H supercomputer located in the Center of Information and Computation, the Tokyo Institute of Technology. Each computation required around 30 s of CPU time.

REFERENCES

1. R. E. Christensen, *SPE J.*, **18,** 571 (1962).
2. J. C. Miller, *SPE Trans.*, **3,** 134 (1963).
3. C. J. Petrie and M. M. Denn, *AIChE J.*, **22,** 209 (1976).
4. J. L. White, *Polym. Eng. Rev.*, **11,** 297 (1981).
5. S. Nam and D. C. Bogue, *Ind. Eng. Chem. Fundam.*, **23,** 1 (1984).
6. T. Matsumoto and D. C. Bogue, *Polym. Eng. Sci.*, **18,** 564 (1978).
7. N. R. Anturkar and A. Co, *J. Non-Newtonian Fluid Mech.*, **28,** 287 (1988).
8. J. D. Tsou and D. C. Bogue, *J. Non-Newtonian Fluid Mech.*, **17,** 331 (1985).
9. R. T. Fisher and M. M. Denn, *AIChE J.*, **22,** 236 (1976).
10. J. R. A. Pearson and M. A. Matovich, *Ind. Eng. Chem. Fundam.*, **8,** 605 (1969).
11. J. R. A. Pearson and Y. T. Shah, *Ind. Eng. Chem. Fundam.*, **13,** 134 (1974).
12. S. Kase, *J. Appl. Polym. Sci.*, **18,** 3279 (1974).
13. H. Ishihara and S. Kase, *J. Appl. Polym. Sci.*, **19,** 557 (1975).
14. G. R. Aird and Y. L. Yeow, *Ind. Eng. Chem. Fundam.*, **22,** 7 (1983).
15. H. I. Freeman and M. J. Coplan, *J. Appl. Polym. Sci.*, **8,** 2389 (1964).
16. C. D. Han and Y. W. Kim, *J. Appl. Polym. Sci.*, **20,** 1555 (1976).
17. J. Cao, *J. Appl. Polym. Sci.*, **42,** 143 (1991).
18. J. Cao, *J. Appl. Polym. Sci.*, **45,** 2169 (1992).
19. S. Kase and T. Matsuo, *J. Polym. Sci. A*, **3,** 2541 (1965).
20. S. Kase and T. Matsuo, *J. Polym. Sci.*, **11,** 251 (1967).
21. K. Toriumi and A. Konda, *Sen-i Gakkaishi*, **40,** 193 (1984).
22. H. Ishihara and S. Kase, *J. Appl. Polym. Sci.*, **20,** 169 (1976).
23. S. Kase and M. M. Denn, in *Proceedings of the 1978 Joint Automatic Control Conference II-71,* Philadelphia, 1978.

Received October 7, 1992
Accepted January 14, 1993